Biochemistry

 Volume 33, Number 45 November 15, 1994

Perspectives in Biochemistry

Analytical Ultracentrifugation of Complex Macromolecular Systems†

Jeffrey C. Hansen,*,‡ Jacob Lebowitz,§ and Borries Demeler‡

Department of Biochemistry, The University of Texas Health Science Center at San Antonio, 7703 Floyd Curl Drive, San Antonio, Texas 78284-7760, and Department of Microbiology, 520 CHSB, University of Alabama at Birmingham, Birmingham, Alabama 35294

Received August 23, 1994

An analytical ultracentrifuge is capable of directly measuring the sedimentation coefficient, *s*, the diffusion coefficient, *D*, and the molecular mass, *M*, of macromolecules ranging in size from several thousand to tens of millions of daltons. When coupled with appropriate data analysis methodologies, it can be used to examine sample purity, detect and characterize conformational changes, determine subunit stoichiometries, characterize assembly and disassembly mechanisms of macromolecular complexes, and measure equilibrium constants and thermodynamic parameters for associating systems. As such, analytical ultracentrifugation is a powerful tool that should be included in the repertoire of any researcher interested in the structure–function relationships of biological macromolecules. Nonetheless, there has been a drastic decline in the use of analytical ultracentrifugation over the last 20 years [see Schachman (1992) for a historical review]. This can be traced almost solely to the fact that functional instrumentation has been unavailable during this period. However, the recent availability of a new state-of-the-art analytical ultracentrifuge, the Beckman XL-A, has reversed this trend. Importantly, the capabilities of the XL-A in most cases have greatly exceeded those of the previous version of the analytical ultracentrifuge, the Beckman Model E. Consequently, analytical ultracentrifugation has not simply been reborn, but has undergone a true metamorphosis. This perspective describes those aspects of this change that most profoundly impact the many biochemists and molecular biologists who currently are unfamiliar with the principles and practice of analytical ultracentrifugation. Namely, it is now possible for a nonexpert to analyze even complex macromolecular systems to a high degree of resolution by advanced calculation-intensive methods with relatively little effort. As a consequence, analytical ultracentrifugation is now approaching the same level of user friendliness and accessibility as, for example, UV–visible spectroscopy.

OVERVIEW OF SEDIMENTATION VELOCITY AND SEDIMENTATION EQUILIBRIUM

An analytical ultracentrifuge can be used to perform two different types of experiments, termed sedimentation velocity and sedimentation equilibrium. Sedimentation velocity experiments measure the velocity and diffusion of a lamella of macromolecules that is formed in solution under the influence of a strong centrifugal field. They are used to determine the *s*, *D*, and in some cases *M*. Sedimentation equilibrium experiments are performed at lower speeds and measure the equilibrium concentration distribution of macromolecules that is formed when the transport by sedimentation is balanced by diffusional transport. They are used to obtain both the *M* of a macromolecule and the thermodynamic parameters for associating systems. This section presents a largely nonmathematical overview of sedimentation velocity and sedimentation equilibrium that is intended to allow the nonexpert to appreciate the powerful data analysis methodologies discussed later in this perspective. Numerous descriptions of the detailed mathematical principles that underlie sedimentation velocity and sedimentation

† Supported by NIH Grants GM45916 and RR08352 (J.C.H.) and P30AI27767 (J.L.).

* Corresponding author. Phone: 210-567-6980. Fax: 210-567-6595. e-mail: hansen@bioc02.uthscsa.edu.

‡ The University of Texas Health Science Center at San Antonio.

§ University of Alabama at Birmingham.

0006-2960/94/0433-13155$04.50/0

equilibrium experiments have been presented previously.[1] Although the equations found in these references often are intimidating to the nonexpert, the availability of sophisticated data analysis programs now allow even a novice to use the analytical ultracentrifuge with confidence.

Sedimentation Velocity. Sedimentation velocity processes are caused by a centrifugal force field acting on a solute particle, leading to movement of the solute toward the bottom of the centrifuge cell. The centrifugal force on the solute is partly counterbalanced by the buoyant force of the displaced solvent. The net sedimentation behavior of macromolecules in a centrifugal field is described by the Svedberg equation:

$$s = \frac{v}{\omega^2 r} = \frac{M(1 - \bar{v}\varrho)}{Nf} \quad (1)$$

The Svedberg relationship indicates that the rate of sedimentation, v, is dependent on several factors: the strength of the centrifugal force field strength, $\omega^2 r$ (where r is the radial distance from the center of rotation); the molecular mass, M; the molecular size and shape (related to the frictional coefficient, f); the density of the solvent, ϱ; and the partial specific volume of the solute, $\bar{v}$. It is important to note that macromolecules in the presence of a centrifugal field not only sediment, but also diffuse. The combination of sedimentation and diffusion in the ultracentrifuge cell is described in terms of the flow, J:

$$J = s\omega^2 rc - D\frac{\partial c}{\partial r} \quad (2)$$

where s is the sedimentation coefficient as described in eq 1, D is the diffusion coefficient, c is the solute concentration, and $\partial c/\partial r$ is the solute concentration gradient. Upon acceleration of the rotor, sedimentation leads to formation of a solute concentration gradient in the form of a boundary or band, and diffusional spreading begins to occur.

Sedimentation velocity measurements in the analytical ultracentrifuge can be made using either band or boundary procedures. Only the latter will be considered in this perspective; descriptions of the former can be found elsewhere.[1] Figure 1A shows a boundary sedimentation velocity experiment, as visualized by the scanning absorption optical system of the XL-A. The centrifuge cell is filled with a solution of macromolecules; at rest the concentration is uniform at all points in the cell and $\partial c/\partial r = 0$. When a sufficient centrifugal force is applied, the macromolecules will move toward the bottom of the cell at a rate proportional to their s. The lamella of macromolecules that was originally present at the meniscus (i.e., the air–solution interface) is referred to as the boundary. Progression of the boundary toward the bottom of the cell leads to the formation of a solute concentration gradient. Except for the boundary region, the solute concentration remains uniform in all other regions of the cell (even though the solutes are moving toward the bottom of the cell at the same rate as the boundary). The small decrease in concentration in the plateau region of successive scans (Figure 1A) is a normal consequence of radial dilution.[1] The diffusional boundary spreading that occurs during a sedimentation velocity experi-

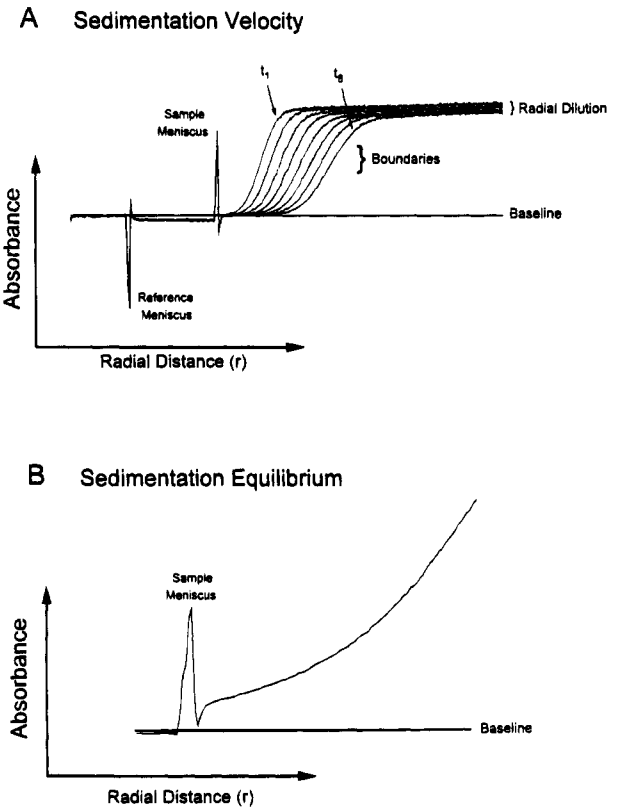

FIGURE 1: (A) Boundary sedimentation velocity experiment. Shown are eight successive scans of a sample of reconstituted oligonucleosomes in low salt buffer [see Schwarz and Hansen (1994)]. The data were collected in digital form using a Beckman XL-A analytical ultracentrifuge equipped with scanning absorption optics. The speed of this run was 20 000 rpm. The direction of sedimentation is from left to right. The scans were collected at ~8-min intervals (the earliest recorded scan is labeled "t_1"; the latest recorded scan is labeled "t_8"). The baseline is the absorbance at which the concentration of the sedimenting sample is zero. The centrifuge cell is composed of two sector shaped compartments, one that holds the sample (e.g., buffer + oligonucleosomes) and one that holds the reference solution (e.g., buffer only). The transmitted intensity at the chosen wavelength is determined in both sectors at ≥0.001-cm radial distance increments by the scanning slit/lens assembly and converted to sample absorbance vs radial distance data (i.e., the "scan"). The radial position of the air–solvent interface in the sample sector is labeled "sample meniscus", while that for the reference sector is labeled "reference meniscus". (B) Sedimentation equilibrium experiment. The same oligonucleosome sample shown in part A was sedimented at 1600 rpm for 72 h. The lower rotor speed resulted in the formation of an equilibrium concentration gradient rather than formation of the moving boundaries illustrated in part A. Equilibrium was achieved as judged by the fact that scans taken at 76–90 h were superimposable with that shown on the figure.

[1] There is a voluminous amount of older literature pertaining to analytical ultracentrifugation that describes in detail much of the information that is addressed only briefly in this perspective. This information is reviewed in the following references: Cantor, C. R., & Schimmel, P. R. (1980) *Biophysical Chemistry, Part II*, W. H. Freeman and Co. San Francisco, CA. Fujita, H. (1975) *Foundations of Ultracentrifugal Analysis*, Wiley, New York. Gilbert, L. M., & Gilbert, G. A. (1973) *Methods Enzymol. 27*, 273–296. Ralston, G. (1993) *Introduction to Analytical Ultracentrifugation*, Beckman Instuments, Fullerton, CA. Schachman, H. K. (1959) *Ultracentrifugation in Biochemistry*, Academic Press, New York. Svedberg, T., & Pedersen, K. O. (1940) *The Ultracentrifuge*, Oxford University Press, Clarendon. Tanford, C. (1961) *Physical Chemistry of Macromolecules* Wiley, New York. Teller, D. C., Swanson, E., & DeHaen, C. (1979) *Methods Enzymol. 61*, 103–124. van Holde, K. E. (1975) in *The Proteins (3rd ed.)* (Neurath, H., & Hill, R. L., Eds.) Vol. 1, pp 225–291, Academic Press, New York. van Holde, K. E. (1985) *Physical Biochemistry*, 2nd ed. Prentice-Hall, Englewood Cliffs, NJ.

ment is indicated clearly in Figure 1A. For simple single component systems, the s traditionally has been determined by measuring the rate of movement of the boundary "midpoint", i.e., the point where the boundary exhibits the steepest positive slope. Methods that allow sedimentation velocity analysis of more complex systems are described below.

Sedimentation Equilibrium. If the centrifugal force is small enough to allow the process of diffusion to significantly oppose the process of sedimentation, and given sufficient time, an equilibrium concentration distribution of macromolecules will be obtained throughout the cell (Figure 1B). For an ideal, single component system that is noninteracting, the concentration distribution is an exponential function of the buoyant mass of the macromolecule, $M(1 - \bar{\nu}\varrho)$, as described by

$$c(r) = c(a) \exp[M(1 - \bar{\nu}\varrho)\omega^2(r^2 - a^2)/2RT] \quad (3)$$

where $c(r)$ is the concentration at radial position r, $c(a)$ is the concentration at the meniscus, a is the radial distance of the meniscus, and R and T represent the gas constant and absolute temperature, respectively. Molecular mass measurements for ideal single component systems traditionally have been made by a linearization of eq 3; the logarithm of $c(r)$ plotted against r^2 yields a slope of $M(1 - \bar{\nu}\varrho)/2RT$. Importantly, if the macromolecular systems are more complex, e.g., are participating in either self- or hetero-associations, or if the solution is thermodynamically nonideal, these factors also will influence the concentration gradient formed in a sedimentation equilibrium experiment. In each of these cases eq 3 has been modified to include these effects,[1] which allows experimental sedimentation equilibrium data to be fit to models that incorporate virtually all combinations of ideality/nonideality, multiple components, and hetero- and self-associations (McRorie & Voelker, 1993).[1]

ADVANCES IN DATA ACQUISITION

The XL-A is an extremely easy instrument to operate. Parameters such as the speed, temperature and duration of the run, the number of scans, and the time between scans each are computer controlled. The sequence of starting the centrifuge, bringing the rotor up to speed, and starting data collection requires a single keystroke; in the case of the Model E, this same sequence of operations required a highly trained and experienced operator. The ease of use of the XL-A ultimately serves to greatly enhance the accessibility of analytical ultracentrifugation to the nonexpert, i.e., within a typical department, both sedimentation velocity and sedimentation equilibrium experiments can be reliably performed by researchers at all levels.[2]

Arguably the single most important advancement of the XL-A is its digital acquisition of $c(r)$ data. The XL-A analytical ultracentrifuge currently comes equipped with a removable high-intensity flash xenon light source/scanning monochromator and a photoelectric detector. This scanning absorption optical detection system can be adjusted to measure the solution absorbance at wavelengths ranging from 190 to 800 nm and at radial distance increments of ≥ 0.001 cm. A real-time Rayleigh interference optical system, which measures the refractive increment between a set of evenly spaced "fringes" to obtain sample concentration, has been developed for existing XL-A's (Laue et al., 1994a). A similar system for the XL-A currently is being developed commercially. For both the absorption and interference optical systems, the $c(r)$ data are recorded directly to a computer hard drive in ASCII code format. The XL-A's digital data acquisition provides the foundation that allows complex multicomponent mixtures to be quickly and easily analyzed by sophisticated data analysis methods.

ADVANCES IN DATA ANALYSIS

The ability to analyze complex macromolecular systems by analytical ultracentrifugation previously was limited to a relatively small number of specialists.[1] Listed below are descriptions of several noteworthy methods that now extend analysis of complex macromolecular systems to the domain of the nonexpert. Importantly, each has been programmed for use with data acquired by the XL-A, and the programs are readily available to potential users in one form or another (in most cases they can be downloaded over the internet from the RASMB anonymous ftp database; see below).

Sedimentation Velocity Methods

In general, sedimentation velocity experiments previously have been analyzed by determining the rate of movement of a single point in the boundaries, e.g., the midpoint or second moment point.[1] Both of these methods yield accurate values of s if the system in question is simple, i.e., consists of a single, noninteracting component. However, the problem with such "single point" methods is that diffusional spreading of the boundaries can hide the presence of multiple components, i.e., the boundaries appear sharp and symmetrical despite being composed of multiple sedimenting species. Analysis of this type of situation by either the midpoint or second moment analysis would yield some type of average s value, rather than the distribution of s that would actually be present. Each of the sophisticated sedimentation velocity methods described in this section was developed at least in part to address this situation.

Extrapolative Determination of the Integral Distribution s. A universally applicable, global boundary analysis method has been developed for use with the absorption optical system by van Holde and Weischet (1978) that determines the integral distribution of s, also known as $G(s)$. The algorithm of the van Holde and Weischet method is based on the fact that sedimentation is proportional to the first power of time, while diffusion is only proportional to the square root of time.[1] Thus, by extrapolation to infinite time, the contribution of diffusion to the boundary shape can be removed.

Analysis by the van Holde and Weischet method of two sets of sharp, symmetrical boundaries is shown in Figure 2. The first step in this method is to divide each scan into n horizontal divisions (usually 20−70) that are evenly spaced between the baseline and the plateau (as opposed to the single division used in the traditional analyses). Using the algorithm described in van Holde and Weischet (1978), an apparent sedimentation coefficient s^*, is calculated from the radial point of each of the n boundary divisions; this results in n values of s^* for each scan. The s^* values are then

[2] A total of 20 different individuals in the Department of Biochemistry at the University of Texas Health Science Center at San Antonio have operated a departmental XL-A over a 2 year period. This includes eight postdoctoral associates, six graduate students, and five technicians.

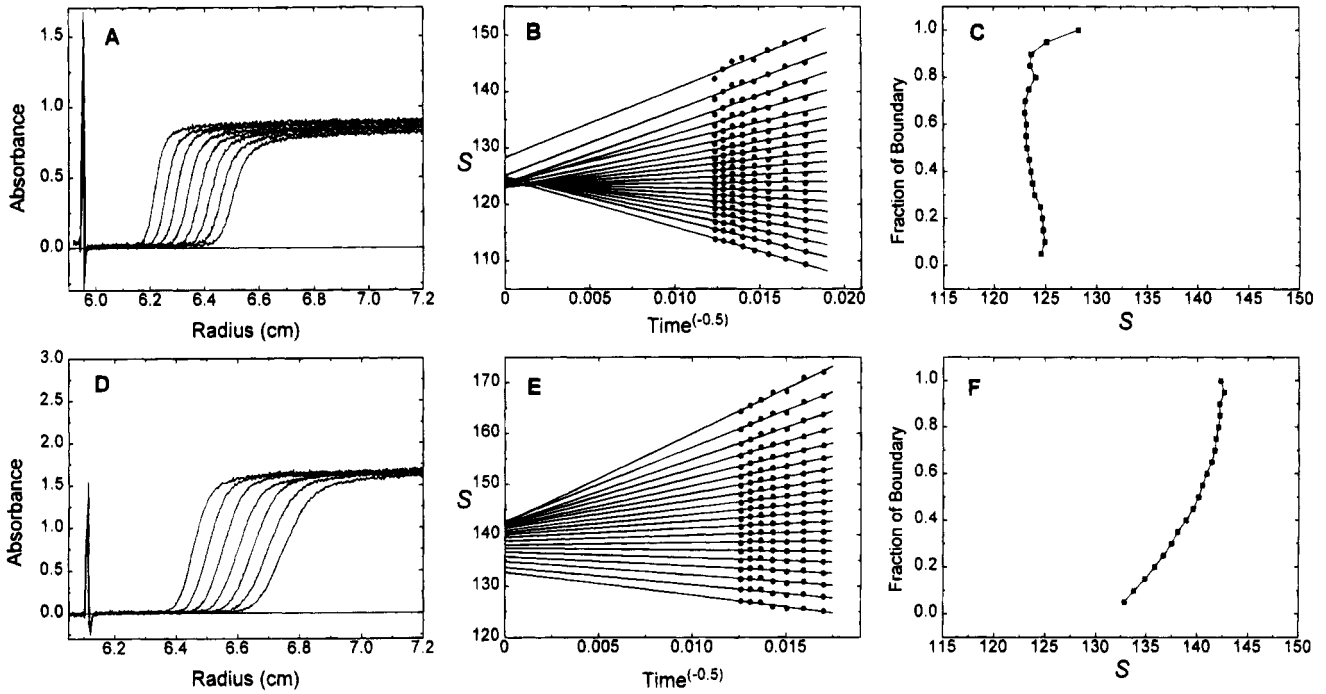

FIGURE 2: Analysis of sedimentation velocity boundaries by the method of van Holde and Weischet (1978). Data were obtained in a Beckman XL-A analytical ultracentrifuge equipped with scanning absorption optics. (Panels A–C) A preparation of bacteriophage T7 MLD capsid II in which <0.01% of the mass of the capsids was subgenomic DNA (Khan et al., 1992). (Panels D–F) A preparation of bacteriophage T7 MLD capsid II in which the capsids contained measurable amounts of subgenomic, packaged DNA (Khan et al., 1992). The boundaries used for the analyses are shown in panels A and D. Extrapolation plots are shown in panels B and E. Integral distribution of s plots is shown in panels C and F. The speed of the run was 10 000 rpm, and the temperature was 20 °C.

plotted vs the inverse square root of the time of each scan, and least-square fits for corresponding s^* values of each scan are performed (Figure 2B,E). The y-intercepts, which correspond to infinite time, yield the diffusion-corrected s at each boundary fraction and together comprise the integral distribution of s. The results are then plotted as boundary fraction vs s. In such a plot, a sample of macromolecules that is homogeneous with respect to both M and f would yield a single y-intercept (Figure 2B) and a vertical s distribution (Figure 2C), while a sample that is heterogeneous with respect to either M or f would yield multiple y-intercepts (Figure 2E) and an s distribution with some type of positive left to right slope (Figure 2F). It has been well-documented that the van Holde and Weischet analysis provides a rigorous test of sample homogeneity (Figure 2; van Holde & Weischet, 1978; Hansen et al., 1989; Gill et al., 1991; Geiselman et al., 1992; Hansen & Lohr, 1993). In addition, and at least of equal importance, it allows one to characterize complex multicomponent systems by sedimentation velocity analysis with confidence (Figure 2D–F; Hansen et al., 1989, 1991; Garcia-Ramirez et al., 1992; Hansen & Lohr, 1993; Hansen & Wolffe, 1994; Mendoza et al., 1994; Schwarz & Hansen, 1994; Behal et al., 1994; Musatov & Robinson, 1994).

The extrapolation plot (Figure 2B,E) also provides a diagnostic for other types of complexity. In several situations, the lines of the plot will cross over before infinite time, i.e., in front of the y-axis. This will occur if the sample either (1) is degraded during the experiment, (2) contains rapidly sedimenting material of heterogeneous s (e.g., aggregates) that decreases the plateau of successive scans beyond that caused by radial dilution, or (3) exhibits a marked concentration dependence of s. Alternatively, parallel lines of negative slope indicate a situation in which a sample is experiencing an increase in s during sedimentation, such as is the case for a slowly aggregating system that has not yet reached equilibrium.

Determination of $g(s)$ from dc/dt. A different extrapolation method for obtaining distributions of s was developed by Stafford (1992a). As with the van Holde and Weischet method, values of s^* are calculated for each radial position. However, in contrast to the van Holde and Weischet method, the time derivative of the concentration distribution is computed at each radial position to produce a differential (rather than integral) distribution of s^*, i.e., $g(s^*)$ (Stafford, 1992b). If desired, the apparent distribution function can then be extrapolated to infinite time to effectively eliminate the effects of diffusion. In this case, the apparent distribution functions obtained at various times are extrapolated to constant values of s^* in the form of $\ln[g(s^*)]$ vs a quadratic function of the inverse square root of time. This avoids extrapolation to negative values of $g(s)$ sometimes observed with the older extrapolation methods.

An advantage of the time derivative method is that the process of differentiation results in the complete elimination of time-independent baseline components, resulting in a considerable increase in the signal-to-noise ratio. In addition, the time derivative patterns can be averaged to provide a further increase in the signal-to-noise ratio (Stafford, 1994a). Because the apparent distribution functions, $g(s^*)$ vs s^*, are nearly geometrically similar to plots of dc/dr vs r, they can reveal details of boundary shape that are not obvious by inspection of the concentration profiles. Therefore, they can often be useful for the analysis of complex systems, even without correction for the effects of diffusion. The large improvements in signal-to-noise ratio obtained by the combination of the time derivative and signal averaging have resulted in about 2–3 orders of magnitude increase in sensitivity depending on the optical system, making this

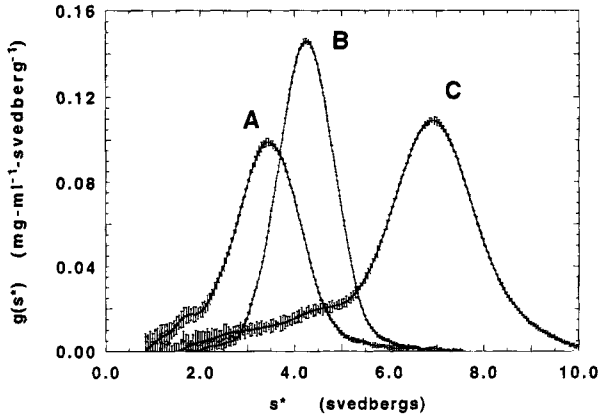

FIGURE 3: Analysis of the interaction of a dimeric single chain antibody fragment with its antigen by the dc/dt sedimentation velocity method. Shown are apparent sedimentation coefficient distribution patterns computed from the time derivative of the concentration profile using the method of Stafford (1992b). These data were collected on a Beckman Model E analytical ultracentrifuge equipped with a video-based Rayleigh optical system. The speed of the run was 56 000 rpm, and the temperature was 20 °C. (A) 0.23 mg/mL 741 F8 $(sFv')_2$. (B) 0.26 mg/mL c-erbB-2 extracellular domain. (C) A mixture of 1.9 μM (0.1 mg/mL) $(sFv')_2$ and 3.8 μM (0.31 mg/mL) c-erbB-2 extracellular domain. Twenty Rayleigh pictures were used. The error bars are the standard error of the mean at each point propagated from the averaged value values of dc/dt. The figure was provided courtesy of Dr. Walter Stafford, III.

method useful for the analysis of complex systems at much lower concentrations than previously possible.

An example of the use of the time derivative method, without any correction for diffusion, is shown in Figure 3. In this example, the interaction of a dimeric single chain Fv antibody ($s^* = 3.3$ S, curve A) with the extracellular domain of the c-erbB-2 oncogene product ($s^* = 4.2$ S, curve B) was studied. Nearly stoichiometric binding of 2 mol of c-erbB-2 extracellular domain to 1 mol of the dimeric antibody fragment was observed after mixing, as judged by both the appearance of a predominantly 6.9 S peak (curve C) and the absence of appreciable amounts of 3.3 S and 4.2 S material. Whereas the apparent distribution functions are of general utility for the routine analysis of both interacting and heterogeneous macromolecular systems (Liu et al., 1994; Laue et al., 1994b; Stafford, 1994b), extrapolation of apparent distribution functions as described above is valid only in the case of heterogeneous systems.

Approximations of the Lamm Equation. Methods have been developed by both Holladay (1979, 1980) and Philo (1994) that fit experimental sedimentation velocity data to models derived from approximations of the Lamm equation (the complex differential equation that fundamentally describes sedimentation velocity processes but that has no general, closed from solution).[1] Under the appropriate conditions, these methods quite accurately determine both s and D. Consequently, one can easily calculate the f, M, and the axial ratio of the molecule without the need for further sedimentation equilibrium experiments. The Philo method globally analyzes up to nine scans and works best in those situations where the boundaries are significantly broadened by diffusion. An important feature of this method is that up to three noninteracting components can be included in the fit. The multicomponent analysis can be applied, for example, to the common situation where protein samples contain some disulfide-linked dimer in addition to the monomeric species and other situations where a small number of discrete components are present that do not interconvert during the course of the experiment. To resolve complex mixtures by this method, the individual components should have s values differing by a factor of ~1.5 or more; its situations where the difference in s values is smaller, the van Holde and Weischet method is preferred. It should be noted that, during multicomponent fitting by this method, the s values are more precisely and uniquely determined than the D values, and it is generally not possible to reliably resolve up to three components unless some of the s and D values are known independently.

Sedimentation Equilibrium Methods

Diagnostics for Complexity. Plots of log c vs r^2, M_{app} vs c, and M_{app} vs r are excellent diagnostics of complexity that can be generated in seconds by a fast desktop computer. If the sample is ideal and monodisperse with respect to M, the slope of the log c vs r^2 plot will be linear. For the other two plots, the M_{app} as a function of c or r will be constant if the sample consists of a single ideal component and will vary if the sample is more complex. One can also determine whether or not the sample is complex by performing a nonglobal nonlinear least-squares fit of a single sedimentation equilibrium c(r) gradient using the equation that describes an ideal single-component situation (eq 3). This model can be fit to a single scan with high confidence (if the baseline c is measured directly at the end of the experiment) since it only has two variable parameters, M and $c_{meniscus}$. A measure of the goodness of the fit is provided by the size and pattern of the χ^2 residuals; for an ideal, single component system the χ^2 residuals will be small and scattered randomly around the fit. The types of deviations expected when eq 3 is used to fit more complex equilibrium concentration gradients are described in McRorie and Voelker (1993).

Although in principle it is possible to derive equilibrium constants from a nonglobal fit of a single data file, for the sake of rigor, analysis of associating systems should be performed by one of the global analysis methods listed below.

Determination of Equilibrium Association Constants for Self-Associating Systems by NONLIN. Yphantis' laboratory has developed a program, designated NONLIN, that performs a global nonlinear least-squares fit of sedimentation equilibrium data (Johnson et al., 1981). This program can be used both to determine the molecular mass (and hence aggregated state) of a macromolecule in solution, as well as for quantitative determination of the association constant-(s), stoichiometries, and nonideality coefficients for self-associating systems (Yphantis & Arakawa, 1987; Dolinnaya et al., 1993; Harbury et al., 1993; Long et al., 1993; Laue, 1994; Liu et al., 1994; Laue et al., 1994b). The NONLIN method is based on the fact that eq 3 can be modified for self-associating systems to a form that contains only the variables $c_{monomer}$, $M_{monomer}$, and the K_a of the n-mer species [see McRorie and Voelker (1993)]. One of the most important parameters to determine for this analysis is the $M_{monomer}$, since convergence to this value must be accurate to achieve a good fit. This can be determined from sequence data or experimentally in the analytical ultracentrifuge in the presence of denaturants. For each curve fitting analysis, one performs a global fit of multiple data files. As alluded to

above, the combination of several sets of data over a wide range of experimental conditions (e.g., different sample loading concentrations and speeds to rotation) is required in order to obtain a unique fit to the data given the number of unfixed variables. The simplest model, a single ideal species, is first examined. If significant self-association occurred, then a poor fit will be obtained and M_1 will not converge on the true $M_{monomer}$. Association models are tested in successive order: monomer−dimer, monomer−trimer, monomer−dimer−trimer, etc. Each fit will yield the value of M_1 and the natural logarithm of the association constant or constants. By constraining a selected K_n to a very low value, one effectively selects the self-association model to be tested. For example, if K_3 is constrained to a negligible value, and K_2 and K_4 are allowed to float, the data are fitted to a monomer−dimer−tetramer model. This illustrates how all combinations of n-mer associations can be examined. The association constants between species, i.e., dimer and trimer and dimer to tetramer, are calculated from the respective K_n values. Acceptance of a satisfactory fit should be judged from the pattern of χ^2 residuals as discussed above and also should be consistent with physical reality.

Analysis of Self-Associating Systems by the Omega Function. The Omega function was introduced by Milthorpe et al. (1975) as a means of avoiding the differentiation step that is required to compute M_{app} in the analysis of association reactions by other methods. Omega (Ω) is defined as a simple, experimentally determinable function of radial position and the measured concentration of associate solute, relative to an arbitrary reference point. Several important types of information relating to self-associating systems can be obtained from Ω vs concentration distributions.

For a reversible self-association reaction that is at equilibrium and without contaminants, the Ω vs concentration distributions from experiments performed at different loading concentrations and at different speeds will overlap. This allows a simple test for both sample homogeneity and attainment of equilibrium; if chemical equilibrium has not been reached (e.g., because of slow association reactions), or if contaminating species are present, the separate concentration distribution curves will not overlap. Furthermore, because the Ω distribution is not distorted by differentiation, it is easier to detect heterogeneity or failure to attain equilibrium (Ralston & Morris, 1992).

The equilibrium association constants for different self-association models, including several "indefinite" or isodesmic schemes, as well as a measure of nonideality, may be estimated from fitting the Ω vs concentration distribution (Morris & Ralston, 1989; Ralston, 1991; Ralston & Morris, 1992). In this context it is interesting to note that while accurate knowledge of the monomer molecular weight is required for accurate assessment of the mode of association and the estimation of the relevant parameters, the test for heterogeneity and failure to attain equilibrium is not particularly sensitive to the value chosen for the monomer molecular weight; any reasonable estimate may be appropriate.

Milthorpe *et al.* (1975) showed that the value of Ω extrapolated to zero concentration allows the calculation of the thermodynamic activity of the monomer at the reference point, from which the thermodynamic activity of the monomer at any other point may be determined. This is particularly useful in studies dealing with high concentrations of solute, in which nonideality may be severe. Extrapolation of the Ω function to zero concentration may be aided by fitting the distribution with appropriate models. This approach has recently been applied in the analysis of self-association of human erythrocyte spectrin (Ralston, 1994), for which independent experiments provided concentrations of several associated species as a function of total concentration. Combination of the two sets of data allowed an assessment of the activity coefficient of the protomer of spectrin as a function of the total concentration.

THE ANALYTICAL ULTRACENTRIFUGATION INTERNET LIST SERVER

One of the most important resources available to potential users of the analytical ultracentrifuge is an internet list server with anonymous ftp database, termed RASMB (for Reversible Associations in Structural and Molecular Biology).[3] There currently are ~100 scientists that communicate regularly through this forum. This includes virtually all of the acknowledged experts in the field of analytical ultracentrifugation, as well as each of the scientists responsible for programming the data analysis method described in this perspective. Since its inception, a variety of topics have been discussed, covering everything from technical problems to software implementation and data interpretation. It is also a software depository. This resource allows users at all levels to quickly get help in all aspects relating to the practice of analytical ultracentrifugation. As such, it plays a key role in allowing the nonexpert user to embrace analytical ultracentrifugation with confidence.

ILLUSTRATIVE PROBLEM-SOLVING EXAMPLES

This section describes specific examples in which one or more of the data analysis methods presented above has been used to address a contemporary research problem. Topics covered include characterization of assembly, disassembly and stability of macromolecular complexes, analysis of macromolecular conformational changes, determination of subunit stoichiometries, and measurement of equilibrium constants and thermodynamic parameters for associating systems. Our intent is to illustrate how "modern" analytical ultracentrifugation can be generally useful to those biochemists and molecular biogists who are interested in the structure/function relationships of complex macromolecular systems.

Analysis of cpn60 Assembly, Disassembly, and Stability Using the van Holde and Weischet Sedimentation Velocity Method. Because s is sensitive to both size and shape, sedimentation velocity experiments are uniquely suited for characterization of the stability of macromolecular assemblies and for identification of the mechanisms by which complex macromolecules are assembled and disassembled. In the latter case, by measuring s distributions in the presence of increasing concentrations of destabilizing agents (e.g., chaotropes, salts), one can identify whether there are discrete dissociation intermediates as well as determine the extent to which the dissociation process is cooperative. This approach has recently been applied to the cpn60 chaperonin complex

[3] One can join RASMB by contacting the system administrator, Dr. Walter Stafford, at the following e-mail address: rasmb-manager-@bbri.eri.harvard.edu. The ftp address for the software depot is bbri.eri.harvard.edu.

by Mendoza et al. (1993). These investigators first sedimented the intact tetradecamers (14-mer of 60-kDa subunits) in the presence of 2.0−2.3 M urea. Analysis of the boundaries by the van Holde and Weischet method indicated that urea in this range induced cooperative dissociation of the 23S tetradecamers into 3S monomers, as judged by the presence of only 3S and 23S species at the intermediate extents of dissociation. However, no dissociation in 2.0−2.3 M urea was observed when the cpn60 complex was prebound with the enzyme rhodanese, indicating that the stability of the cpn60 complex was greatly enhanced by binding of a single small protein substrate. Finally, it was observed that incubation of dissociated cpn60 in 2.75−3.0 M urea with unfolded rhodanese led to noncooperative reassembly of some 3−12S intermediates and some intact 23 S tetradecamers.

Analysis of Salt-Dependent Chromatin Folding Using the van Holde and Weischet Sedimentation Velocity Method. Chromatin, which is the genetic material of eukaryotes, is a conformationally dynamic protein−nucleic acid assembly. The sequential folding of chromatin from an extended structure to a highly condensed structure has been implicated in both chromosome formation and regulation of transcription. However, the contributions of the core histones to the chromatin folding process long have remained obscure. To address this question, Schwarz and Hansen (1994) studied the influence of $MgCl_2$ on the sedimentation behavior of a 12-mer oligonucleosome model system composed of only core histones and DNA. Both in the absence and presence of $MgCl_2$, the resulting sedimentation velocity boundaries appeared sharp and symmetrical. However, analysis by the van Holde and Weischet method indicated that whereas the oligonucleosomes in the absence of salt sedimented as a single 29S species, there was a heterogeneous distribution of species that sedimented between 35 and 55S in the presence of $MgCl_2$. Importantly, both the midpoint and second moment analyses gave apparent values in $MgCl_2$ of only ~45S. Sedimentation equilibrium experiments performed in the absence and presence of $MgCl_2$ in both cases yielded an oligonucleosome molecular mass of 3×10^6 daltons. Cumulatively, the sedimentation data indicated that the increases in s in $MgCl_2$ resulted from formation of a population of folded oligonucleosome structures, the maximum of which sedimented at the 52S expected for a higher order solenoidal conformation. Only through analysis of the deceptively complex boundaries by the van Holde and Weischet method was it possible to conclude that the core histones alone can direct formation of higher order chromatin structures. In contrast, analysis by either of the single point methods, or by any other biophysical technique that measures *average* behavior, would have led to the erroneous conclusion that the oligonucleosomes were incapable of forming such highly folded structures.

The experiments of Schwarz and Hansen (1994) describe a situation in which the observed heterogeneity in s resulted entirely from heterogeneity in f. It should be noted that the data obtained with bacteriophage T7 capsids (Figure 2D−F) illustrate the opposite situation, i.e., in this case the observed heterogeneity in s presumably resulted entirely from heterogeneity in M due to the presence of different amounts of subgenomic DNA within the capsid particles.

Determination of Bacteriophage λ cI Repressor Stoichiometry by NONLIN. It has long been thought that λ cI repressor dimers cooperatively associate into tetramers when bound to adjacent sites on operator DNA and that assembly of the tetramer complex is an important step in transcriptional control [see Ptashe (1992) for a review]. The association state of bacteriophage λ cI repressor dimers has recently been determined by NONLIN global analysis of sedimentation equilibrium data (Laue et al., 1993; Senear et al., 1993). Quite unexpectedly, these data unequivocally demonstrated that the stable associated state of the repressor is an octamer, both before and after binding to operator DNA. These studies beautifully illustrate the importance of rigorously determining subunit stoichiometry by analytical ultracentrifugation. While accessibility problems generally have precluded application of analytical ultracentrifiguation to many complex macromolecular systems, this no longer need be the case.

Sedimentation Equilibrium Analysis of HIV-1 Reverse Transcriptase Heterodimer Stability. HIV-1 reverse transcriptase (RT) converts the viral genome from single-stranded RNA into double-stranded DNA, which is then integrated into the cellular genome. The active form of RT is a heterodimer composed of 66-kDa (p 66) and 51-kDa (p51) polypeptides, where p51 is a proteolytic product of p66. RT is a proposed target for the treatment of acquired immunodeficiency syndrome; hence it is important to understand the strength and stability of the subunit−subunit interactions required for RT activity. On the basis of the apparent lack of dissociation of RT during HPLC gel exclusion chromatography, Restle et al. (1990) estimated that the K_a for the p66−p51 interactions was $\geq 10^9$ at 0 °C. The large K_a value suggests that the RT heterodimer is quite stable. However, the sedimentation equilibrium analyses of Becerra et al. (1991) and Lebowitz et al. (1994) each yielded dimerization K_a values of only 5×10^5 at 5 °C, which indicates that the RT heterodimer is in fact only moderately stable. It should be noted that the latter studies treated the p66−p51 interaction as a pseudo self-association reaction and used NONLIN to fit the sedimentation equilibrium data to a monomer−dimer−trimer/tetramer model, while the former studies fit the data to an independently developed monomer−dimer heteroassociation model. Nonetheless, both approaches yielded an identical dimerization K_a value at 5 °C. These results demonstrate the importance of measuring equilibrium association constants by a thermodynamically rigorous method such as sedimentation equilibrium.

Integrated Analysis of Biglycan Self-Association Using NONLIN and the dc/dt Method. The recent work of Liu et al. (1994) provides a beautiful example of how a complex self-associating system can be analyzed by integrated use of both sedimentation velocity and sedimentation equilibrium experiments. Biglycan is a proteoglycan that contains two dermatan sulfate chains attached to a 37-kDa protein core. It is found in the extracellular matrix of connective tissues and both binds to, and regulates the function of, other extracellular matrix proteins such as TGFβ and fibronectin. The sequence of experiments employed by Liu et al. (1994) was as follows. Standard sedimentation velocity analyses indicated that monomeric biglycan (2.9S) forms 4.8S and 9.4S species in nondenaturing buffer lacking or containing Zn^{2+}, respectively. Standard sedimentation equilibrium experiments performed in the absence of Zn^{2+} indicated that thermodynamic nonideality obscures determination of M at high concentrations but suggested that formation of the 4.8S species appeared to result from mass-action-driven dimer-

ization at lower concentrations. To confirm this interpretation, sedimentation velocity experiments were performed at very low biglycan concentrations using an XL-A equipped with a prototype interference optical system (Laue et al., 1994a), and data were analyzed by the d*c*/d*t* method. Results were consistent with those predicted by Gilbert theory[1] for a rapid monomer−dimer equilibrium. In the presence of Zn^{2+}, both the NONLIN-derived *z*-average molecular weight and the d*c*/d*t*-derived *s* distributions indicated that biglycan existed predominantly as a hexamer. Upon establishment of this complex behavior for the native biglycan, these investigators used similar approaches to establish that only the protein core of biglycan is capable of self-association.

Determination of the Thermodynamic Parameters for Spectrin Self-Association Using the Ω Function. The utility of the Ω function is best illustrated by the detailed analysis of the self-association of spectrin by Ralston's laboratory. Spectrin is a major cytoskeletal protein present on the cytoplasmic side of the erythrocyte membrane. It is a conformationally dynamic $\alpha\beta$-heterodimer that undergoes self-association to form tetramers and higher order aggregates. Whereas self-association has been qualitatively documented by several techniques including nondenaturing gel electrophoresis, only sedimentation equilibrium has been able to quantitatively analyze the association mechanism with rigor. Morris and Ralston (1989) and Ralston (1991) used the Ω function to show that spectrin self-associated could be best modeled by an indefinite association scheme in which the K_a of the dimerization of the spectrin protomer was different than that for binding of the protomer to existing oligomers. Their analysis further indicated that the weight fraction of higher oligomers present in solution under equilibrium conditions was substantially greater than had been observed by the electrophoretic studies performed under nonequilibrium conditions. By measuring the K_a as a function of temperature to determine the $\Delta H°$, $\Delta S°$, and $\Delta C_p°$ for the association reaction, a thermodynamic model was developed that describes how spectrin self-association behavior relates to its biological function in the erythrocyte membrane (Ralston, 1991).

FUTURE PROSPECTS

At the beginning of this decade, the future of analytical ultracentrifugation was bleak. Model E's had completely disappeared from use, save for those in the laboratories of a few dedicated experts. Almost inconceivably, just a few short years later analytical ultracentrifugation has reemerged as a technique that can be used effectively and with great benefit by virtually any contemporary researcher. There are still several hurdles that must be overcome before analytical ultracentrifugation can again reach its full potential. Most notably, the several generations of younger scientists that are almost completely unaware of the utility of this technique must be reeducated, and the principles of analytical ultracentrifugation must again become standard fare in biophysical chemistry courses. Also, the XL-A must become as widely available as was the model E (there were over 1500 Model E's in use in its heyday).

Over the next several years there will be continued advances in both in the areas of instrumentation development and data analysis methodologies. In the latter case, this will involve continued conversion of many of the previously established analysis methods[1] into user friendly software, including those involving hetero-associations of macromolcules (Rivas & Minton, 1993; Kim et al., 1994). In terms of instrumentation, progress will occur in areas such as development of a fluorescence detection system for the XL-A (T. Laue, personal communication). Perhaps most exciting of all will be the inevitable infusion of new ideas and applications that will result from the "rediscovery" of analytical ultracentrifugation by the next generations of scientists.

ACKNOWLEDGMENT

We are indebted to Drs. John Philo, Greg Ralston, and Walter Stafford, III, for their invaluable contributions to the text, and to Dr. Paul Horowitz for critically reading the manuscript. We thank Dr. Philip Serwer for providing the bacteriophage capsids that were analyzed in Figure 2 and Dr. Walter Stafford, III, for providing Figure 3. This perspective is dedicated to our mentors, Drs. K. E. van Holde and the late J. Vinograd, who taught us the problem-solving approach to analytical ultracentrifugation.

REFERENCES

Becerra, S. P., Kumar, A., Lewis, M. S., Widen, S. G. Abbotts, J., Karawya, E. M., Hughes, S. H., Shiloach, J., & Wilson, S. H. (1991) *Biochemistry 30*, 11707−11719.

Behal, R. H., DeBuysere, M. S., Demekv, B., Hansen, J. C., & Olson, M. S. (1994) *J. Biol. Chem.* (in press).

Dolinnaya, N. G., Braswell, E. H., Fossella, J. A., Klump, H., & Fresco, J. R. (1993) *Biochemistry 32*, 10263−10270.

Garcia-Ramirez, M., Dong, F., & Ausio, J. (1992) *J. Biol. Chem. 267*, 19587−19595.

Geiselmann, J., Yager, T. D., Gill, S. C., Camettes, P., & von Hippel, P. H. (1992) *Biochemistry 31*, 111−121.

Gill, S. C., Yager, T. D., & von Hippel, P. H. (1991) *J. Mol. Biol. 220*, 325−333.

Hansen, J. C., & Lohr, D. (1993) *J. Biol. Chem. 268*, 5840−5848.

Hansen, J. C., & Wolffe, A. P. (1994) *Proc. Natl. Acad. Sci. U.S.A. 91*, 2339−2343.

Hansen, J. C., Ausio, J., Stanik, V. H., & Van Holde, K. E. (1989) *Biochemistry 28*, 9129−9136.

Hansen, J. C., van Holde, K. E., & Lohr, D. (1991) *J. Biol. Chem. 266*, 4276−4282.

Harbury, P. B., Zhang, T., Kim, P. S., & Alber, T. (1993) *Science 262*, 1401−1406.

Holladay, L. A. (1979) *Biophys. Chem. 10*, 187−190.

Holladay, L. A. (1980) *Biophys. Chem. 11*, 303−308.

Johnson, M. L., Correia, J. J., Yphantis, D. A., & Halvorson, (1981) *Biophys. J. 36*, 575−588.

Khan, S., Griess, G., & Serwer, P. (1992) *Biophys. J. 63*, 1286−1292.

Kim, S. J., Tsukiyama, T., Lewis, M. S., & Wu, C. (1994) *Protein Sci. 3*, 1040−1051.

Laue, T. M. (1994) *Methods Enzymol.* (in press).

Laue, T. M., Senear, D. F., Eaton, S., & Ross, J. B. A. (1993) *Biochemistry 32*, 2469−2472.

Laue, T. M., Anderson, A. L., & Demaine, P. D. (1994a) *Prog. Colloid Polym. Sci. 94*, 74−81.

Laue, T. M., Starovasnick, M. A., Klevit, R. E., & Weintraub, H. (1994b) *Proc. Natl. Acad. Sci. U.S.A.* (in press).

Lebowitz, J., Kar, S., Braswell, E., McPherson, S., & Richard, D. L. (1994) *Protein Sci.* (in press).

Liu, J., Laue, T. M., Choi, H. U., Tang, L.-H., & Rosenberg, L. (1994) *J. Biol. Chem.* (in press).
Long, C. G., Braswell, E., Zhu, D., Apigo, J., Baum, J., & Bodsky, B. (1993) *Biochemistry 32*, 11688−11695.
McRorie, D. K., & Voelker, P. J. (1993) *Self-Associating Systems in the Analytical Ultracentrifuge*, Beckman Instruments, Inc., Fullerton, CA.
Mendoza, J. A., Demeler, B., & Horowitz, P. M. (1994) *J. Biol. Chem. 269*, 2447−2451.
Milthorpe, B. K., Jeffrey, P. D., & Nichol, L. W. (1975) *Biophys. Chem. 3*, 169−176.
Morris, M. B., & Ralston, G. B. (1989) *Biochemistry* 8561−8567.
Musatov, A., & Robinson, N. C. (1994) *Biochemistry* (in press).
Philo, J. (1994) in *Modern Analytical Ultracentrifugation: Acquisition and Interpretation of Data for Biological and Synthetic Polymer Systems* (Shuster, T. M., Laue, T. M., & Eds.) pp 156−170, Boston, Birkhauser, Boston.
Ptashne, M. (1992) *A Genetic Switch*, 2nd ed., Cell Press & Blackwell Science Publications, Cambridge, MA.
Ralston, G. B. (1991) *Biochemistry 30*, 4179−4186.
Ralston, G. B. (1994) *Biophys. Chem.* (in press).
Ralston, G. B., & Morris, M. B. (1992) in *Analytical Ultracentrifugation in Biochemistry and Polymer Science* (Harding, S. E., Rowe, A. J., & Horton, J. C., Eds.) pp 253−274, Royal Society for Chemistry, Cambridge, U.K.
Restle, T., Muller, B. & Goody, R. S. (1990) *J. Biol. Chem. 265*, 8986−8988.
Rivas, G., & Minton, A. P. (1993) *Trends Biochem. Sci. 18*, 284−287.
Schachman, H. K. (1992) in *Analytical Ultracentifugation in Biochemistry and Polymer Science* (Harding, S. E., Rowe, A. J., & Horton, J. C., Eds.) pp 3−15, Royal Society for Chemistry, Cambridge, U.K.
Schwarz, P. M., & Hansen, J. C. (1994) *J. Biol. Chem. 269*, 16284−16289.
Senear, D. F., Laue, T. M., Ross, J. B. A., Waxman, E., Eaton, S., & Rusinova, E. (1993) *Biochemistry 32*, 6179−6189.
Stafford, W. F. (1992a) in *Analytical Ultracentrifugation in Biochemistry and Polymer Science* (Harding, S. E., Rowe, A. J., & Horton, J. C., Eds.) pp 359−393, Royal Society for Chemistry, Cambridge, U.K.
Stafford, W. F. (1992b), *Anal. Biochem. 203*, 295−301.
Stafford, W. F. (1994a) *Methods Enzymol.* (in press).
Stafford, W. F. (1994b) in *Modern Analytical Ultracentrifugation: Acquisition and Interpretation of Data of Biological and Synthetic Polymer Systems* (Shuster, T. M., & Laue, T. M., Eds.) pp 119−137, Boston, Birkhauser, Boston.
van Holde, K. E., & Weischet, W. O. (1978) *Biopolymers 17*, 1387−1403.
Yphantis, D. A., & Arakawa, T. (1987) *Biochemistry 26*, 5422−5427.